Striatal Dopamine Transporter Imaging in Nonhuman Primates with Iodine-123-IPT SPECT

Robert T. Malison, Janet M. Vessotskie, Mei-Ping Kung, William McElgin, Gemma Romaniello, Hee-Joung Kim, Mark M. Goodman and Hank F. Kung

Department of Psychiatry, Yale University School of Medicine, New Haven, Connecticut; Department of Radiology, University of Pennsylvania School of Medicine, Philadelphia, Pennsylvania; and Department of Radiology, University of Tennessee Medical Center, Knoxville, Tennessee

The regional distribution, kinetics and pharmacological specificity of a new radioiodinated cocaine analog, N-((E)-3-iodopropen-2-yl)-2β-carbomethoxy-3β-(4-chlorophenyl) tropane ([^{123}I]IPT) were examined in brain SPECT studies (n = 20) of nonhuman primates. **Methods:** Radiolabeling and purification of the iododestannylated trialkyltin precursor yielded the tracer at greater than 90% radiochemical purity and high (>20,000 Ci/mmole) specific activity. Cynomologous monkeys were injected with 7.2 ± 1.3 mCi (mean ± s.d.) of the tracer, and serial 10-min images were acquired (total scan time = 177 ± 22 min). Images were reconstructed as transaxial slices (2 mm) using restorative techniques (Wiener prefiltering). **Results:** Radioactivity concentrated quickly in striatal regions (time of peak = 25 ± 13 min) and cleared gradually thereafter (8.8 ± 4.6 %/hr). Striatal-to-cerebellar ratios of 2.6 ± 1.5 (n = 19), 6.7 ± 3.2 (n = 20), 15.1 ± 10.7 (n = 10) and 22.8 ± 11.0 (n = 9) were observed at the time of peak and at 1, 2 and 3 hr p.i., respectively. In contrast, extrastriatal activity peaked earlier and at lower levels, cleared more rapidly and resembled cerebellar time-activity curves. Displacing doses of nonspecific antagonists of monoamine transporters (mazindol and β-CIT) showed that 95% of specific [^{123}I]IPT binding was reversible, while selective antagonists (e.g., paroxetine, nisoxetine and GBR 12909) demonstrated that striatal activity was specifically associated with dopamine transporters. **Conclusion:** These results indicate that [^{123}I]IPT is a useful radioligand for in vivo SPECT imaging of striatal dopamine transporters.

Key Words: iodine-123-IPT; dopamine transporters; single-photon emission computed tomography

J Nucl Med 1995; 36:2290–2297

Located on the terminal axons of dopamine neurons, the dopamine transporter (i.e., reuptake site) is a presynaptic carrier protein which serves to remove neurotransmitter from the synaptic cleft following its release, thereby terminating the chemical communication between nerve cells and recycling the residual neurotransmitter (*1*). Pharmacological antagonism of the dopamine transporter appears to play a central role in both the addictive properties of cocaine (*2*) and the therapeutic actions of certain antidepressant medications (*3*). In vitro studies in postmortem human brain have also suggested its importance as a marker for monitoring and/or understanding the pathophysiology of a variety of neuropsychiatric disorders, including cocaine abuse (*4*), Tourette's syndrome (*5*) and Parkinson's disease (*6,7*). As a result, much interest exists in the in vivo assessment of the dopamine transporter in clinical populations. In fact, functional radiotracer techniques, including PET and SPECT, have recently demonstrated dopamine transporter loss in Parkinson's disease (*8,9*).

A variety of radiopharmaceuticals for the dopamine transporter have been developed as potential PET and SPECT imaging agents (*10–17*). Among these, recently synthesized analogs of cocaine, in which a phenyltropane moiety substitutes for the benzoyl ester linkage, have been shown to bind to the dopamine transporter with higher affinity, lower nonspecific binding and greater metabolic stability than cocaine itself. Such agents include WIN 35,428 (also known as CFT) (*8,18*), β-CIT (methyl 3β-(4-iodophenyl)tropane-2β-carboxylate) (also known as RTI-55) (*19,20*) and IP-CIT (also known as RTI-121) (*21*). In their various radiolabeled forms, these newer agents have offered improvements over prior radiopharmaceuticals with respect to their greater target-to-background ratios and their enhanced brain retention in vivo. Despite these improvements, ongoing research has focused on the development of structurally related derivatives with yet improved signal-to-noise characteristics, more rapid brain kinetics, and greater selectivity for binding to the dopamine as opposed to the serotonin (5-HT) transporter.

Recently, Goodman et al. reported on a phenyltropane derivative of cocaine in which a nitrogen-substituted iodovinyl group was exploited as an alternative radiolabeling scheme (*22*) (Fig. 1). In its radioiodinated form, N-((E)-3-[^{125}I]iodopropen-2-yl)-2β-carbomethoxy-3β-(4-chlorophenyl) tropane ([^{125}I]IPT) appeared to be a particularly promising ligand for the dopamine transporter based on in vitro

Received Nov. 2, 1994; revision accepted Mar. 12, 1995.

For correspondence contact: Robert T. Malison, MD, Department of Psychiatry, Yale University School of Medicine, 34 Park St., New Haven, CT 06519.

For reprints contact: Hank F. Kung, PhD, University of Pennsylvania School of Medicine, 3700 Market St., Room 305, Philadelphia, PA 19104.

and in vivo studies in the rodent. The purpose of the current investigation was to characterize the regional distribution, kinetics and pharmacological specificity of [^{123}I]IPT brain uptake in nonhuman primates using SPECT as an initial step towards establishing its utility as an in vivo imaging agent for the dopamine transporter in humans.

MATERIALS AND METHODS

Radiolabeling

High specific activity (>20,000 Ci/mmole) [^{123}I]IPT was prepared by iododemetalation of the corresponding tributylstannyl precursor as previously described (*22*). Hydrogen peroxide (50 μl, 3% w/v), hydrochloric acid (50 μl, 0.1 N) and no-carrier-added [^{123}I]sodium iodide (5 μl, specific activity ≈ 200,000 Ci/mmole) were added to a septum-sealed vial containing the tin substrate (50 μg/50 μl ethanol). After 30 min, peroxidation was interrupted by adding sodium bisulfite (100 μl, 300 mg/ml) and adjusting the pH to 8.5 with saturated sodium bicarbonate. The reaction mixture was extracted with ethyl acetate (1 × 3 ml), dried by an annhydrous sodium sulfate column (0.2 × 5 cm) and evaporated under a nitrogen stream. The resulting residue was dissolved in ethanol (50 μl, 100%) for reverse-phase HPLC purification using an isocratic solvent system (93% acetonitrile, 7% 5 m*M* 3,3-dimethylglutaric acid buffer, pH = 7.0; flow 1.0 ml/min; retention time 11–12 min). Combined ethyl acetate extracts of the effluent were concentrated under nitrogen and reconstituted in ethanol, yielding (50%–60% overall) the final product at >90% radiochemical purity. Iodine-123-IPT was diluted in normal (0.9%) saline, sterile-filtered and determined to be pyrogen-free prior to studies in nonhuman primates.

Animal Preparation

A series of 20 SPECT imaging studies were conducted in six male cynomologous monkeys (4.0–5.6 kg). Following an overnight fast, animals were immobilized with a combined intramuscular injection of ketamine (10 mg/kg) and xylazine (2 mg/kg). Anesthesia was maintained by passive inhalation of 1.5% isoflurane in oxygen. Endotracheal intubation and subcutaneous glycopyrrolate (2 μg/kg), a peripherally acting anticholinergic agent, minimized risks of aspiration. Core body temperature was kept at >37°C, and vital signs (heart rate and respirations) were monitored every 30 min by an indwelling esophageal stethoscope. An intravenous line in a superficial saphenous vein allowed maintenance hydration (0.9% NaCl, 2 cc kg^{-1} hr^{-1}) as well as radioisotope and drug administration. Animals were placed in a cylindrical polycarbonate "cradle" equipped with an individualized foam head-holder (Smithens Medical Products, Inc.; Tallmadge, OH) to enable reproducible head fixation for imaging in the canthomeatal plane.

SPECT

Experiments were performed on the Picker PRISM 3000 (Bedford Heights, OH), a triple-head SPECT camera equipped with low-energy, high-resolution (LEHR) fanbeam collimators. In this configuration, the instrument's tomographic in-plane resolution was determined to be 10.95 mm (FWHM) based on the point-spread function of an ^{123}I line source in scattering medium. Following intravenous injection of 7.2 ± 1.3 mCi [^{123}I]IPT, monkeys underwent serial 10-min SPECT scans for 177 ± 22 min (range 120–240) using a symmetrical 20% ^{123}I energy window (i.e., 159 ± 16 keV), a 128 × 128 matrix, 120 projections over 360° and a magnification factor of 1.78. Individual image acquisitions were reconstructed using restorative techniques (i.e., a count-dependent two-dimensional Wiener prefilter) (*23*). Images were displayed as 2.0-mm thick transaxial slices having pixel dimensions of 1.11 × 1.11 mm, resulting in a final voxel volume of 2.46 mm^3. Attenuation correction was performed by first-order approximation (*24*), assuming uniform attenuation (μ = 0.10) within elipses fit to brain contours on a slice-by-slice basis.

The regional distribution and temporal kinetics of [^{123}I]IPT brain uptake were established in a series of control experiments (n = 10) after the administration of radiotracer alone. Concentrations of radioactivity were determined for multiple brain areas (e.g., right and left striatum, hypothalamus/midbrain, occipital cortex and cerebellum) using native PRISM 3000 software. By summing the first six 10-min image acquisitions, a composite (i.e., 60 min) image was obtained on which region of interest (ROI) templates were created. Striatal and occipital ROIs were placed on the same transaxial slice as determined by the brightest striatal profile. Midbrain and cerebellar templates were positioned at separate brain levels based on maximal activity and brain contour, respectively. Nonidentical, albeit highly uniform ROI areas (mean ± s.d. pixels) were achieved across studies for the right (98 ± 21) and left striatum (95 ± 19), midbrain (55 ± 11), occipital cortex (233 ± 38) and cerebellum (275 ± 80). Templates were then applied to corresponding slices of individual image acquisitions to obtain regional measures of relative radioactive density (counts min^{-1} pixel^{-1}) over time.

Pharmacologic Displacements

The reversibility and pharmacological specificity of regional [^{123}I]IPT binding was determined by displacement studies (n = 10) in which nonradioactive drugs were administered 90 min postinjection of radiotracer. Various agents were examined, including nonselective monoamine reuptake inhibitors (i.e., mazindol, 4.7 μmole kg^{-1}; β-CIT, 0.9 μmole kg^{-1}) (*25–27*); selective antagonists of dopamine (GBR 12909, 3.4 and 7.6 μmole kg^{-1}) (*28*), serotonin (paroxetine, 3.1 μmole kg^{-1}) (*29,30*) and norepinephrine (nisoxetine 3.0 μmole kg^{-1}) (*31*) transporters, D_1 (SCH23390, 3.7 μmole kg^{-1}) (*32*) and $D_{2/3}$ (raclopride, 1.8 μmole kg^{-1}) (*33*) dopamine receptor antagonists and the mixed dopamine releaser/reuptake inhibitor (d-amphetamine, 2.7 μmole kg^{-1}). The effects of increases in endogenous neurotransmitter (i.e., dopamine) on radiotracer binding were assessed by an infusion of L-DOPA (252 μmole kg^{-1} over 15 min) preceded (60 min) by a bolus injection of benserazide (5 mg kg^{-1} or 20.7 μmole kg^{-1}), a peripherally acting DOPA decarboxylase inhibitor.

Data Analysis

The time needed to reach peak [^{123}I]IPT uptake was determined for individual brain regions in both control and pharmacological displacement experiments. Striatal activity was analyzed as the weighted (by ROI area) average of bilateral count densities. Ratios of striatal-to-cerebellar activities provided estimates of the ligand's in vivo signal-to-noise properties at early (i.e., peak and 1 hr p.i.; all studies) and late (2 and 3 hr p.i.; control studies only) imaging times. Basal (i.e., postpeak) and drug-induced (i.e., post-displacer) rates of brain [^{123}I]IPT washout were calculated as the percent change per hour (as estimated by linear regression) relative to peak or predisplacer levels, respectively. Values are cited as the mean ± s.d.

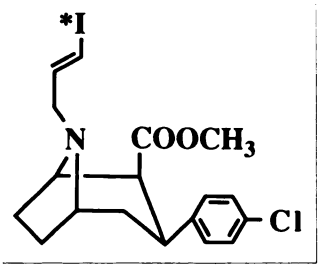

FIGURE 1. The chemical structure of [^{123}I]IPT.

RESULTS

Regional Distribution and Kinetics

Iodine-123-IPT distributed rapidly and globally throughout the brain on the initial (0–10 min) SPECT image, consistent with a pattern of cerebral blood flow. By 20–30 min p.i., imaged activity visibly concentrated in striatal regions bilaterally. Although extrastriatal activity appeared uniform on individual 10-min scans, composite (i.e., 0–60 min summed) images suggested a discrete area of midline [^{123}I]IPT uptake of similar intensity to occipital and cerebellar regions (Fig. 2). This area of so-called "hypothalamic/midbrain" activity was located roughly 4–6 slices (8–12 mm) below the level of maximal striatal uptake.

Iodine-123-IPT achieved peak concentrations in the striatum by 25 ± 13 min and cleared gradually thereafter (8.8 ± 4.6 %/hr, n = 10). In contrast, activity in extrastriatal regions, including the hypothalamus/midbrain, occipital cortex and cerebellum, peaked earlier, attained lower peak levels and cleared more quickly (Table 1). The kinetics of [^{123}I]IPT uptake and clearance in extrastriatal regions were comparable. In fact, radiotracer binding in hypothalamic/midbrain and occipital regions closely resembled time-activity curves for the cerebellum (Fig. 3). Despite a steady decline in striatal [^{123}I]IPT activity after 30 min, striatal-to-cerebellar ratios continued to climb, equaling 2.6 ± 1.5 (n = 19), 6.7 ± 3.2 (n = 20), 15.1 ± 10.7 (n = 10) and 22.8 ± 11.0 (n = 9) at the time of peak and at 1, 2 and 3 hr p.i., respectively. In contrast, ratios for hypothalamus/midbrain and occipital cortex remained close to unity for the duration of the control studies (Table 2).

Test-Retest Experiments

Four cynomologous monkeys underwent two control studies each to establish the variability in striatal washout rates across animals and the test-retest reliability of washout within animals. Washout rates averaged 9.4 ± 4.7 %/hr (n = 8 experiments; range 2.8–13.7 %/hr) in the four monkeys (Table 3). A comparison of test and retest scans demonstrated a mean absolute difference in washout rates of 2.3 ± 2.3 %/hr (range 0.3–4.8 %/hr), indicating a lesser degree of variability in striatal [^{123}I]IPT clearance for studies performed within an animal. For reasons unclear, reproducibility appeared to be better for animals having faster washout rates (absolute difference = 0.3–0.4 %/hr).

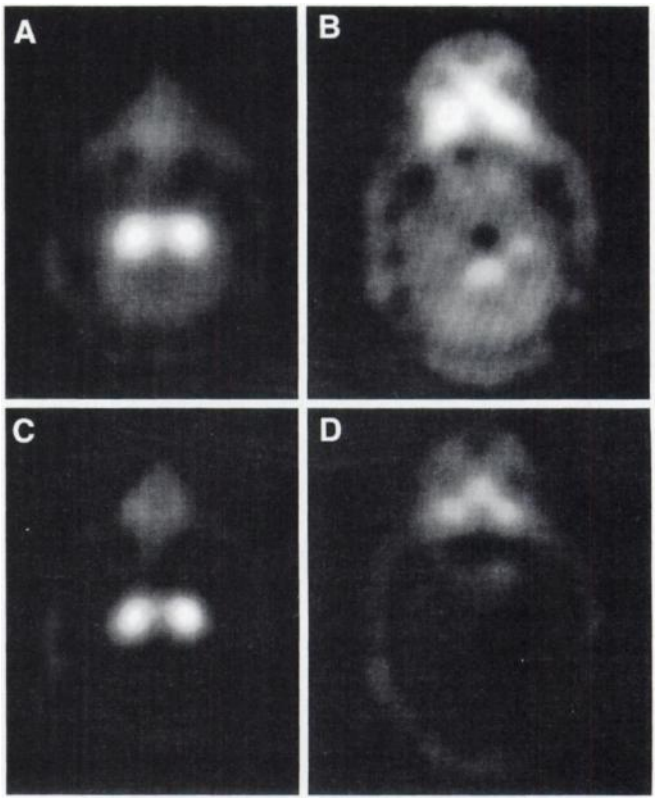

FIGURE 2. Two pairs of transaxial slices taken from composite 0–60 min (A and B) and 120–180 min (C and D) SPECT images from a control experiment in a cynomologous monkey after the injection of 5.5 mCi [^{123}I]IPT. The in vivo distribution of [^{123}I]IPT brain activity at the level of the striatum and occipital cortex (A and C) and the hypothalamus/midbrain and cerebellum (B and D) are depicted. The highest concentrations of [^{123}I]IPT activity were observed in the striatal regions, with a faint region of early (0–60 min) midline (designated as hypothalamus/midbrain) activity (B). Extracranial activity in the nose was non-displaceable.

Pharmacologic Displacement Studies

Given the reasonably slow rates of striatal washout (≤13.7%/hr), it was possible to assess the in vivo specificity of [^{123}I]IPT binding in striatum by measuring the change in washout induced by individual displacing drugs. Similar assessments were not possible for midbrain and occipital regions due to the rapid clearance of tracer at early times

TABLE 1
Summary of Regional Iodine-123-IPT Kinetics*

Region	Time to Peak (Minutes)	Peak Activity (% Striatum)	Washout† (%/hr)
Striatum	25 ± 13	100	9 ± 7
Hypothalamus/ Midbrain	11 ± 3	78 ± 6	71 ± 12
Occipital cortex	11 ± 3	70 ± 14	72 ± 13
Cerebellum	10 ± 0	80 ± 12	74 ± 12

*Values expressed as the mean ± s.d.
†Calculated for the hour following peak uptake.

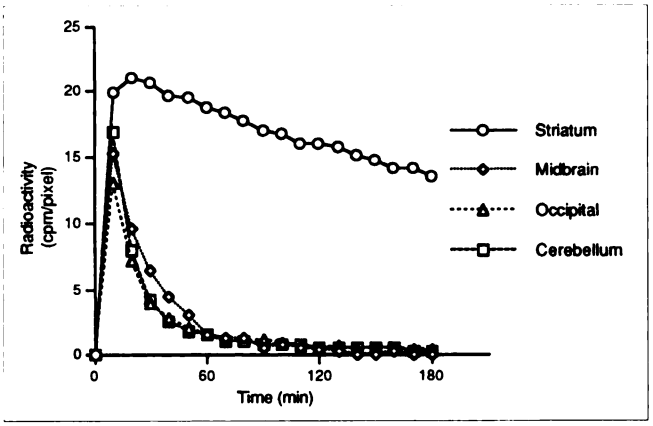

FIGURE 3. Regional time-activity curves for striatum, midbrain, occipital cortex and cerebellum from the experiment depicted in Figure 2. Striatal activity peaked by 20 min after radiotracer injection and washed out gradually thereafter (13.7 %/hr). In contrast, extrastriatal (i.e., midbrain, occipital and cerebellar) activity peaked early (by 10 min p.i.) at lower levels and cleared much more rapidly.

(30–90 min) and the low levels of residual activity at later times (>90 min). Given the variability in tracer washout across animals (Table 3) and the impracticality of performing all displacement studies in a single animal, pharmacologically-induced changes in the brain clearance of [^{123}I]IPT were determined relative to basal clearance rates within the same experiment. Specifically, the percent change per hour in [^{123}I]IPT binding was calculated for the 60 min preceding (i.e., 30–90 min p.i.) and the 60 min following (i.e., 90–150 min p.i.) the administration of displacing agents. The net change (Δ %/hr) in *clearance* (i.e., not transporter occupancy) was obtained by subtracting the predrug from postdrug washout rates and provided a qualitative, albeit objective, means of establishing whether a given agent displaced [^{123}I]IPT binding. Changes in brain washout were examined over identical intervals for nondisplacement (i.e., control) studies as well to assess normal differences in early compared to late washout rates.

Nonspecific antagonists of monoamine transporters, including mazindol and β-CIT, produced robust reductions in [^{123}I]IPT binding as indicated by net changes in striatal washout (i.e., Δ %/hr) of 47.8 and 83.0%/hr, respectively.

TABLE 2
Regional Brain Activity Ratios over Time

Region	Activity ratio (region/cerebellum)*			
	Peak†	1 hr†	2 hr‡	3 hr‡
Striatum	2.6 ± 1.5	6.7 ± 3.2	15.1 ± 10.7	22.8 ± 11.0
Hypothalamus/ Midbrain	1.0 ± 0.1	1.4 ± 0.3	1.1 ± 0.3	0.7 ± 0.5
Occipital cortex	0.9 ± 0.1	1.0 ± 0.1	1.0 ± 0.1	1.1 ± 0.2

*Mean ± s.d.
†Control and displacement studies.
‡Control studies only.

TABLE 3
Test-Retest Differences in Striatal Iodine-123-IPT Washout (Percent Change/Hour)

Animal No.	Test	Retest	Absolute difference
5522	6.3	2.8	3.5
5521	8.7	3.9	4.8
5053	13.2	13.5	0.3
2093	13.7	13.3	0.4
Mean ± s.d.	9.4	2.3	
	4.7	2.3	

Displacements were dramatic, as depicted by changes in striatal time-activity curves following β-CIT (Fig. 4). In contrast, highly selective norepinephrine, serotonin and dopamine reuptake inhibitors demonstrated variable effects (Fig. 5). Nisoxetine, an agent with selective affinity at the norepinephrine transporter alone (*31,34*) failed to induce any noticeable change in [^{123}I]IPT washout (Δ %/hr = 0.0). Similarly, the selective serotonin reuptake inhibitor paroxetine had little effect on [^{123}I]IPT washout, with postdisplacer rates increasing only marginally (1.0%/hr). Values for nisoxetine and paroxetine were well within the range of values determined from all nondisplacement studies (−1.9 ± 3.8 %/hr; range −9.7 to 4.1%/hr; n = 10) and the range of control values calculated from a single experiment in each of the five monkeys in whom displacements were performed (−0.3 ± 2.9 %/hr; range −3.0 to 4.1 %/hr; n = 5). In stark contrast to nisoxetine and paroxetine, the highly selective dopamine transporter antagonist GBR 12909 caused clear dose-dependent increases in striatal [^{123}I]IPT clearance or 24.0 and 83.3%/hr for low (3.4 μmole kg^{-1}) and high (7.6 μmole kg^{-1}) doses, respectively. As was the case for nonselective antagonists (i.e., mazindol and

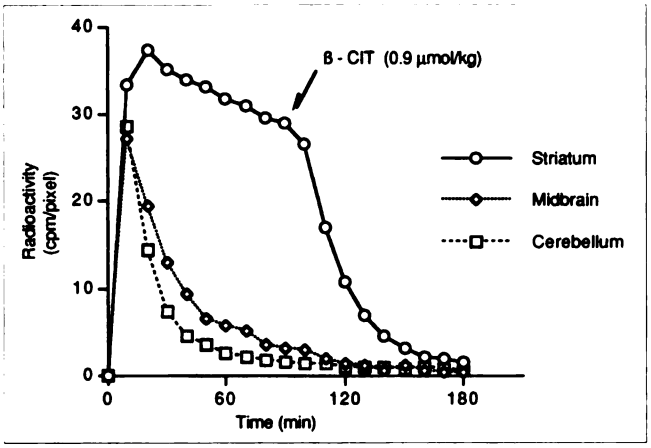

FIGURE 4. Pharmacological displacement of striatal [^{123}I]IPT uptake by the nonselective monoamine reuptake inhibitor β-CIT (i.e., RTI-55; 0.9 μmole/kg i.v.). Baseline (30–90 min) washout rates in striatum (18 %/hr) increased to 101 %/hr after β-CIT, a net change in [^{123}I]IPT washout of 83 %/hr. Specific (i.e., striatal-cerebellar) [^{123}I]IPT binding was reduced by ~95% (calculated as [$Specific_{90}$-$Specific_{180}$]/$Specific_{90}$ * 100), suggesting that the vast majority of [^{123}I]IPT binding is reversibly bound to monoamine transporters.

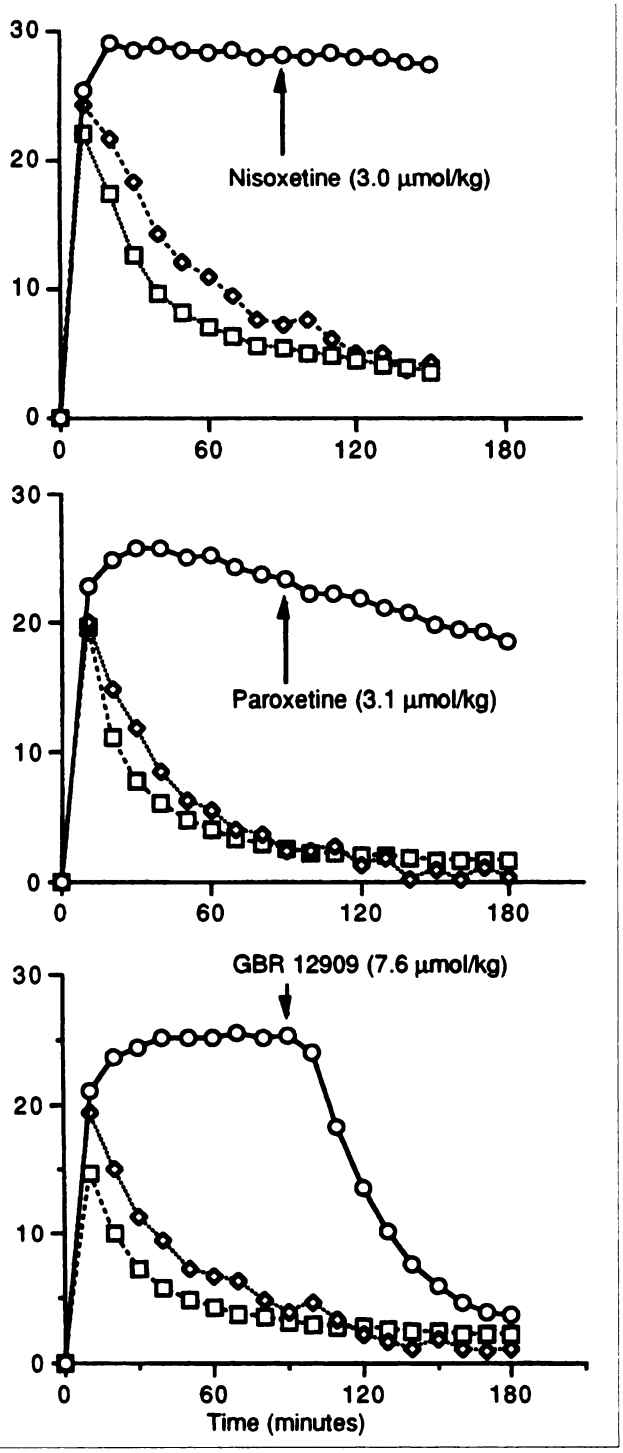

FIGURE 5. The effects of selective norepinephrine (NE), serotonin (5-HT) and dopamine (DA) transporter antagonists on brain [^{123}I]IPT uptake. Nisoxetine (3.0 μmole/kg i.v.), a selective norepinephrine reuptake inhibitor, and paroxetine (3.1 μmole/kg i.v.), a highly selective serotonin transporter antagonist, failed to increase [^{123}I]IPT washout rates in the striatum (net changes = 0 %/hr and 1 %/hr, respectively). In contrast, GBR 12909 (7.6 μmole/kg i.v.), a highly selective antagonist at the dopamine transporter, dramatically decreased specific striatal [^{123}I]IPT binding ([$Specific_{90}$-$Specific_{180}$]/$Specific_{90}$ * 100 = 94%), suggesting that striatal [^{123}I]IPT activity is exclusively associated with the dopamine transporter. Reductions in specific binding were consistent with the robust differences in pre- (0 %/hr) versus postdisplacer (83%/hr) washout.

β-CIT), the magnitude of change in washout rates for GBR 12909 easily exceeded the 99% confidence interval (i.e., 3 s.d.) for control values. Although the mixed dopamine releaser/reuptake inhibitor d-amphetamine produced reductions in [^{123}I]IPT binding (35.2%/hr), an infusion of l-DOPA appeared to have no effect (0.5%/hr). Nor were significant changes in [^{123}I]IPT washout produced by SCH23390 (−0.5%/hr) or raclopride (−4.4%/hr), dopamine D_1 and $D_{2/3}$ receptor antagonists, respectively. Results from these pharmacological displacement studies are summarized in Figure 6.

DISCUSSION

This study demonstrates the utility of [^{123}I]IPT for imaging striatal dopamine transporters in nonhuman primates with SPECT. While other iodinated probes for the dopamine transporter have been described (*10,16,26,35,36*), [^{123}I]IPT may provide significant advantages over currently available SPECT tracers given its superior target-to-background ratio, reversible binding, rapid brain kinetics and apparent pharmacological specificity for dopamine transporter sites in vivo. As such, [^{123}I]IPT is a particularly promising candidate for clinical investigations in human subjects.

Regional Distribution

Iodine-123-IPT attained high concentrations in monkey striatum, while much lower levels of activity were observed in extrastriatal regions (Fig. 2). Ratios of striatal-to-cerebellar activity as measured by our SPECT camera were 15.1 at 2 hr and 22.8 at 3 hr p.i. Such values are the highest reported to date for any dopamine transporter imaging agent, including ratios for [^{123}I]β-CIT/RTI-55 (7.3 at 5 hr and 12 at 21 hr p.i.) (*19,20*), [^{11}C]CFT/WIN 35,428 (2.5–3.0 at 2 hr p.i.) (*18*) and [^{123}I]IP-β-CIT/RTI 121 (7.0 at 3.2 hr p.i.) (*21*) in nonhuman primates. The excellent contrast of [^{123}I]IPT is consistent with work in the rat in which in vivo ratios of basal ganglia-to-cerebellar activities reached 16:1 by 1 hr after injection (*22*). Reasons for [^{123}I]IPT's relatively enhanced signal-to-noise characteristics are not entirely clear, since other tropane congeners possess comparable in vitro affinity for striatal binding sites in rats (*37*). Thus, other factors such as ligand lipophilicity and in vivo metabolism may help to explain the differences between radiopharmaceuticals. Both affinity and lipophilicity have been demonstrated to influence target-to-background ratios for $D_{2/3}$ receptor radioligands (*38*). Since absolute uptake (percent dose/gram of tissue) of [^{123}I]IPT in rat whole brain (0.13 ± 0.02 at 120 min) and basal ganglia (0.61 ± 0.07 at 120 min) was only modest, low levels of nonspecific binding may account for the high striatal-to-cerebellar ratios. Of note, encouraging preliminary results in humans suggest a similarly robust ligand signal (striatal/cerebellar activity = 26 at 3 hr (*39*).

Tracer Reversibility

Despite steadily increasing striatal-to-cerebellar ratios (Table 2), [^{123}I]IPT satisfies both pharmacologic and kinetic criteria for a reversibly binding tracer in vivo. Nonspecific antagonists of monoamine transporters (i.e., mazindol and β-CIT) produced dramatic displacements of

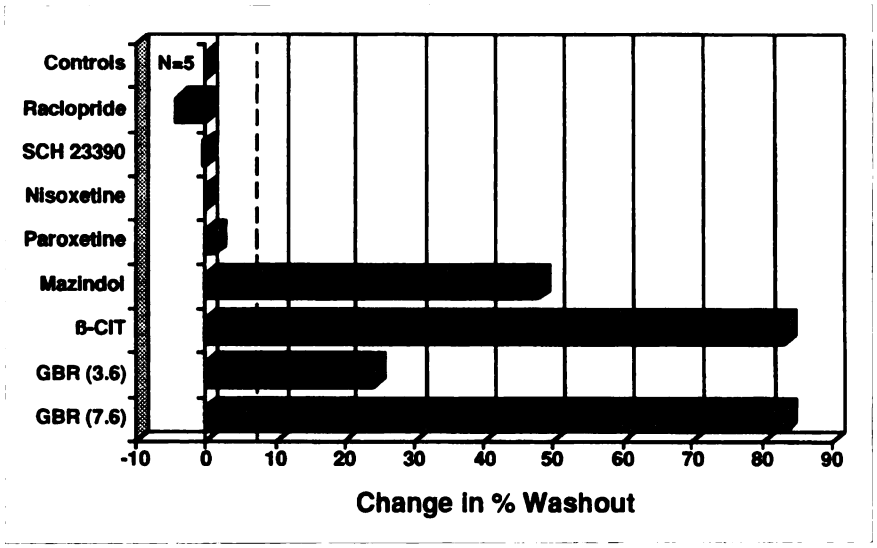

FIGURE 6. A bar graph summarizing the results of pharmacological displacement experiments in five cynomologous monkeys. Horizontal bars indicate the net change (%/hr) in striatal [^{123}I]IPT clearance, as derived by subtracting pre- (30–90 min) from postdisplacer (90–150 min) washout rates. Results from individual displacement studies are compared to the mean ± s.d. (−0.3 ± 2.9) values from control experiments (n = 5) in the same animals. The dashed line denotes a level of change in [^{123}I]IPT washout of 3 s.d. above that observed for control studies.

[^{123}I]IPT binding from the striatum. Changes in washout were visually unambiguous (Fig. 3) and statistically distinct (3 s.d.) from control values (Fig. 6). For β-CIT (Fig. 4), specific (i.e., striatal-cerebellar) [^{123}I]IPT binding after displacement (i.e., 180 min p.i.) was reduced to ~5% of preinjection (i.e., 90 min p.i.) levels, a value essentially equivalent to background (i.e., cerebellar) values. In contrast, no discernible change in cerebellar activity was observed, arguing against a nonspecific influence of displacers on peripheral tracer metabolism. This near complete reversibility of [^{123}I]IPT binding indicates that the vast majority (~95%) of specific striatal activity is associated with transporter binding sites. In addition, the comparable levels of postdisplacement activity in striatum and cerebellum suggests the suitability of using the latter region as a measure of nonspecific binding during in vivo imaging studies.

In addition to pharmacologic reversibility, [^{123}I]IPT behaves in a kinetically reversible fashion as well. Striatal [^{123}I]IPT activity peaked by 30 min in all but two experiments, clearing at a steady rate (~9% per hour) postpeak. The presence of ascending and descending components to striatal time-activity curves suggests in vivo phases of net association and dissociation, respectively (*40*). Thus, [^{123}I]IPT may lend itself to a variety of model-based methods for measuring dopamine transporter levels in vivo, including tracer kinetic, graphical and equilibrium (e.g., peak, transient and sustained/constant infusion) approaches (*40*). Such versatility allows for the cross-validation of outcome measures obtained by alternate approaches, as previously demonstrated with the SPECT $D_{2/3}$ receptor radioligand [^{123}I]iodobenzofuran (i.e., [^{123}I]IBF) (*41,42*).

Pharmacological Specificity

A major aim of this study was to characterize the pharmacologic nature of striatal [^{123}I]IPT binding in vivo. Like cocaine and various other phenyltropane analogs (e.g., β-CIT, CFT) (*27,43–48*), [^{123}I]IPT possesses in vitro affinity for both dopamine and serotonin transporters. Prior work in rodent tissue homogenates has shown that [^{123}I]IPT binds with high affinity to transporters for both dopamine (K_d = 0.3 n*M*) and serotonin (K_d = 2.1 n*M*) (M-P Kung, personal communication). Although the highest concentrations of dopamine transporters are found in the striatum (*49*), modest levels of striatal serotonin reuptake sites also exist (*50*). Thus, our displacement studies were specifically designed to determine whether striatal [^{123}I]IPT activity was primarily associated with dopamine or serotonin reuptake sites.

As noted above, dramatic displacements of [^{123}I]IPT binding were observed for mazindol and β-CIT. Both agents are nonselective in their actions at monoamine reuptake sites. Mazindol potently inhibits dopamine, serotonin and norepinephrine uptake, possessing half-maximum (i.e., IC_{50}) inhibition values of 18, 30 and 0.65 n*M*, respectively (*51*). Similarly, β-CIT has been well characterized in vitro and shows nanomolar affinity for both dopamine ($K_{d\,high}$ = 0.2n*M*; $K_{d\,low}$ = 5.8n*M*) and serotonin (K_d = 0.2 n*M*) transporters (*27*). In contrast to these nonselective agents, the diphenyl-substituted piperazine derivative, GBR 12909, has been shown to have greater selectivity for inhibiting dopamine as compared to serotonin (~170 fold) and norepinephrine (~440 fold) uptake (*28*). Injections of 3.4 and 7.6 μmole/kg produced dose-dependent increases in striatal [^{123}I]IPT washout. For the highest dose, GBR displaced 94% of specific [^{123}I]IPT binding in striatum (Fig. 5), equalling the 95% reduction seen with β-CIT. Consistent with near total displacement of [^{123}I]IPT by GBR 12909 was the absence of any effect of serotonin- and norepinephrine-selective agents. Paroxetine, a greater than 10,000 fold more potent serotonin than dopamine reuptake inhibitor (*51*), produced no noticeable displacement of [^{123}I]IPT binding. Similarly, the highly selective norepinephrine transporter antagonist nisoxetine (*31,34*) showed no evidence of change in [^{123}I]IPT washout. Taken together, these displacement data strongly suggest that striatal [^{123}I]IPT activity is almost exclusively (~95%) associated with dopamine transporter sites in vivo.

The apparent in vivo specificity of [^{123}I]IPT binding,

while unexpected, may be explained by prior work with [^{125}I]IPT, cocaine and related phenyltropane imaging agents. First, our imaging data are consistent with in vitro studies performed with [^{125}I]IPT in the rat. Competition binding data demonstrate a rank order potency for inhibiting basal ganglia [^{125}I]IPT binding which parallel antagonist affinity for the dopamine transporter (*22*). Similarly, in vitro studies in human (*52*) and nonhuman (*53*) primate brain suggest that [^{3}H]cocaine recognition sites in the striatum are principally associated with the dopamine transporter, despite cocaine's known affinity for other monoamine reuptake sites (*2*). Lastly, in vivo imaging studies in monkeys using radiolabelled β-CIT demonstrate a similar regional selectivity for the dopamine transporter (*20,54*). Specifically, β-CIT activity in striatum appeared to be exclusively associated with the dopamine transporter despite clear evidence of serotonin transporter binding in extrastriatal regions. Thus, one possible explanation for the in vivo specificity of [^{123}I]IPT is a predominance of dopamine over serotonin reuptake sites in the striatum. Alternatively, in vitro measures of ligand affinity may not always reliably predict transporter binding in vivo (*55*).

Despite [^{123}I]IPT's clear pharmacologic reversibility, it is noteworthy that l-DOPA administration failed to change [^{123}I]IPT washout in the striatum. The doses chosen have been shown to result in plasma l-DOPA concentrations of 5–15 μg/ml in baboons (*20*), levels above those found to ameliorate Parkinson's disease symptoms (*56*). Thus, [^{123}I]IPT binding may be relatively immune to changes in endogenous dopamine levels. Since the mixed dopamine releaser/transporter antagonist d-amphetamine produced substantial changes in [^{123}I]IPT binding, we cannot exclude the possibility that more dramatic elevations in extracellular dopamine might have an effect. For the dose of d-amphetamine used, microdialysis studies in vervet monkeys have suggested changes on the order of 40-fold (Bradberry CW, *personal communication*).

Extrastriatal Activity

Among other brain regions, only activity in the hypothalamus/midbrain attained levels above those observed in the cerebellum. Ratios were increased transiently (at 60 min) and marginally (1.4 ± 0.3) above unity in control studies (Table 2). While visual inspection of time-activity curves at times suggested an effect of displacers (Fig. 5), no objective differences in activity ratios were found when displacement studies were compared to values obtained in control experiments. As a result, the pharmacological nature of [^{123}I]IPT binding in this region is unclear. Serotonin reuptake sites are widely distributed in the brain, including a variety of diencephalic and mesencephalic nuclei (e.g., thalamus, hypothalamus, substantia nigra, superior and inferior colliculi and the dorsal raphe) (*57–61*). In addition, considerable numbers of dopamine reuptake sites are known to exist in extrastriatal regions such as the substantia nigra (*62*). Thus, the low levels of activity in this region could reflect binding to either dopamine or serotonin transporters. Alternatively, a higher degree of nonspecific binding cannot be excluded. Reports on in vivo imaging studies using [^{11}C]β-CIT PET (*54*) and [^{123}I]β-CIT SPECT (*20*) have noted significant degrees of "thalamic" or "hypothalamic/midbrain" binding, respectively. Pharmacological characterization of this extrastriatal activity by both groups has suggested its association with the serotonin transporter. Whether the relatively lower levels of [^{123}I]IPT activity observed in this region are due to its lesser affinity for the serotonin transporter (2.1 versus 0.2 n*M* in vitro), an increase in partial volume effects as a result of using smaller primates (*20*) or a lower resolution instrument (*54*) or other in vivo factors (*38,55*) remains to be determined.

CONCLUSION

We have shown that [^{123}I]IPT is a promising new SPECT ligand for imaging striatal dopamine transporters in nonhuman primates. Its extremely favorable target-to-background binding, reversible kinetics and pharmacological specificity in vivo make it an attractive addition to currently available radiopharmaceuticals for the dopamine transporter. Studies in human subjects are underway (*39*) and should help to establish the ligand's ultimate suitability for studies of clinical populations.

ACKNOWLEDGMENTS

The principal investigator (RTM) conducted these studies with the support of a Department of Veterans Affairs Substance Abuse Research Fellowship, a National Institute on Drug Abuse Institutional Research Scientist Development Award and a National Alliance for Research on Schizophrenia and Depression (NARSAD) Young Investigator Award.

REFERENCES

1. Rudnick G, Clark J. From synapse to vesicle: the reuptake and storage of biogenic amine neurotransmitters. *Biochim Biophys Acta* 1993;1144:249–263.
2. Ritz M, Lamb R, Goldberg S, Kuhar M. Cocaine receptors on dopamine transporters are related to self-administration of cocaine. *Science* 1987;237: 1219–1223.
3. Kapur S, Mann J. Role of the dopamine system in depression. *Biol Psychiatry* 1992;32:1–17.
4. Little K, Kirkman J, Carroll F, Clark T, Duncan G. Cocaine use increases [^{3}H]WIN 35428 binding sites in human striatum. *Brain Res* 1993;628:17–25.
5. Singer H, Hahn I, Moran T. Tourette's syndrome: abnormal dopamine uptake sites in postmortem striatum from patients with Tourette's syndrome. *Ann Neurol* 1991;30:558–562.
6. Janowsky A, Vocci F, Berger P, et al. [^{3}H]GBR 12935 binding to the dopamine transporter is decreased in the caudate nucleus in Parkinson's disease. *J Neurochem* 1987;46:617–621.
7. Kaufman M, Madras B. Severe depletion of cocaine recognition sites associated with the dopamine transporter in Parkinson's diseased striatum. *Synapse* 1991;9:43–49.
8. Frost J, Rosier A, Reich S, et al. Positron emission tomographic imaging of the dopamine transporter with ^{11}C-WIN 35,428 reveals marked declines in mild Parkinson's disease. *Ann Neurol* 1993;34:423–431.
9. Innis R, Seibyl J, Scanley B, et al. Single-photon emission computed tomographic imaging demonstrates loss of striatal dopamine transporters in Parkinson disease. *Proc Natl Acad Sci USA* 1993;90:11965–11969.
10. Basmadjian G, Mills S, Kanvinde M, Basmadjian N. Structure biodistribution relationship of radioiodinated tropeines: search for a molecular probe for the characterization of the cocaine receptor. *J Lab Compd Radiopharm* 1990;28:801–810.
11. Ding Y, Fowler J, Volkow N, et al., Synthesis of [^{11}C]dl-threo-methylphenidate: drug pharmacokinetics and binding to the presynaptic neuron. *10th*

International Symposium on Radiopharmaceutical Chemistry, Kyoto, Japan, October 25–28, 1993.
12. Fowler J, Volkow N, Wolf A, et al. Mapping cocaine binding sites in human and baboon brain in vivo. *Synapse* 1989;4:371–377.
13. Kilbourn M, Haka M, Mulholland G, Jewett D, Kuhl D. Synthesis of radiolabeled inhibitors of presynaptic monoamine uptake systems: [^{18}F]GBR 13119 (DA), [^{11}C]nisoxetine (NE), and [^{11}C]fluoxetine (5-HT). *J Lab Compd Radiopharm* 1989;26:412.
14. Leenders K, Salmon E, Tyrrell P, et al. The nigrostriatal dopaminergic system assessed in vivo by PET in healthy volunteer subjects and patients with Parkinson's disease. *Arch Neurol* 1990;47:1290–1298.
15. Müller L, Halldin C, Farde L, et al. Carbon-11-β-CIT, a cocaine analogue—preparation, autoradiography and preliminary PET investigations. *Nucl Med Biol* 1993;20:249–255.
16. Yu D, Gatley S, Wolf A, et al. Synthesis of carbon-11 labeled iodinated cocaine derivatives and their distribution in baboon brain measured using positron emission tomography. *J Med Chem* 1992;35:2178–2183.
17. Maziere B, Coenen H, Halldin C, Nagren K, Pike V. PET radioligands for dopamine receptors and re-uptake sites—chemistry and biochemistry. *Nucl Med Biol* 1992;19:497–512.
18. Wong DF, Yung B, Dannals RF, et al. In vivo imaging of baboon and human dopamine transporters by positron emission tomography using [^{11}C]WIN 35,428. *Synapse* 1993;15:130–42.
19. Shaya E, Scheffel U, Dannals R, et al. In vivo imaging of dopamine reuptake sites in the primate brain using single-photon emission computed tomography (SPECT) and iodine-123 labeled RTI-55. *Synapse* 1992;10:169–172.
20. Laruelle M, Baldwin R, Malison R, et al. SPECT imaging of dopamine and serotonin transporters with [^{123}I]β-CIT: pharmacological characterization of brain uptake in nonhuman primates. *Synapse* 1993;13:295–309.
21. Scheffel U, Dannals RF, Wong DF, Yokoi F, Carroll FI, Kuhar MJ. Dopamine transporter imaging with novel, selective cocaine analogs. *Neuroreport* 1992;3:969–72.
22. Goodman M, Kung M, Kabalka G, Kung H, Switzer R. Synthesis and characterization of radioiodinated N-(3-iodopropen-2-yl)-2β-carbomethoxy-3β-(4-chlorophenyl)tropanes: potential dopamine reuptake site imaging agents. *J Med Chem* 1994;37:1535–1542.
23. Parker J. *Image reconstruction in radiology*. Boca Raton, FL: CRC Press; 1990.
24. Chang L. A method for attenuation correction in computed tomography. *IEEE Trans Nucl Sci* 1987;25:638–643.
25. Javitch J, Blaustein R, Snyder S. Tritiated mazindol binding associated with neuronal dopamine and norepinephrine uptake sites. *Mol Pharmacol* 1984; 26:35–44.
26. Neumeyer J, Wang S, Milius R, et al. [Iodine-123-]2-B-carbomethoxy-3-B-(4-iodophenyl)tropane: high-affinity SPECT radiotracer of monoamine reuptake sites in brain. *J Med Chem* 1991;34:3144–3146.
27. Boja J, Mitchell W, Patel A, et al. High-affinity binding of [^{125}I]RTI-55 to dopamine and serotonin transporters in rat brain. *Synapse* 1992;12:27–36.
28. Andersen P. The dopamine uptake inhibitor GBR 12909: selectivity and molecular mechanism of action. *Eur J Pharmacol* 1989;166:493–504.
29. Habert E, Graham D, Tahraoui L, Claustre Y, Langer S. Characterization of [^{3}H]paroxetine binding to rat cortical membranes. *Eur J Pharmacol* 1985; 118:107–114.
30. Marcusson J, Bergström M, Eriksson K, Ross S. Characterization of [^{3}H]paroxetine binding in rat brain. *J Neurochem* 1986;50:1783–1790.
31. Tejani-Butt S. [^{3}H]Nisoxetine: a radioligand for quantitation of norepinephrine uptake sites by autoradiography or by homogenate binding. *J Pharmacol Exp Ther* 1992;260:427–36.
32. Hyttel J. SCH23390—the first selective dopamine D-1 antagonist. *Eur J Pharmacol* 1983;91:153–154.
33. Landwehrmeyer B, Mengod G, Palacios JM. Differential visualization of dopamine D2 and D3 receptor sites in rat brain. A comparative study using in situ hybridization histochemistry and ligand binding autoradiography. *Eur J Neurosci* 1993;5:145–53.
34. Tejani-Butt S, Brunswick D, Frazer A. Tritiated nisoxetine: a new radioligand for norepinephrine uptake sites in brain. *Eur J Pharmacol* 1990;191:239–43.
35. Baldwin R, Zea-Ponce Y, Al-Tikriti M, et al. Regional brain uptake and pharmacokinetics of [^{123}I]N-w-fluoroalkyl-2β-carboxy-3β-(4-iodophenyl)-nortropane esters in baboons. *Nucl Med Biol* 1994;22:211–219.
36. Carroll F, Gao Y, Rahman M, et al. Synthesis, ligand binding, QSAR and CoMFA study of 3β-(p-substituted phenyl)tropane-2β-carboxylic acid methyl esters. *J Med Chem* 1991;34:2719–2725.
37. Carroll F, Lewin A, Boja J, Kuhar M. Cocaine receptor: biochemical characterization and structure-activity relationships of cocaine analogues at the dopamine transporter. *J Med Chem* 1992;35:969–981.
38. Kessler R, Ansari M, de Paulis T, et al. High affinity dopamine D2 receptor radioligands. 1. Regional rat brain distribution of iodinated benzamides. *J Nucl Med* 1991;32:1593–1600.
39. Mozley P, Kim H, Stubbs J, et al. Brain and cardiac uptake of I-123 IPT: an analog of cocaine [Abstract]. *J Nucl Med* 1994;35:129P.
40. Malison R, Laruelle M, Innis R. Positron and single-photon emission tomography: principles and applications in psychopharmacology. In: Kupfer D, Bloom F, eds. *Psychopharmacology: the fourth generation of progress*. New York: Raven; 1994:865–879.
41. Laruelle M, van Dyck C, Abi-Dargham A, et al. Compartmental modeling of iodine-123-iodobenzofuran binding to dopamine D2 receptors in healthy subjects. *J Nucl Med* 1994;35:743–754.
42. Kung M-P, Kung H, Billings J, Yang Y, Murphy R, Alavi A. The characterization of IBF as a new selective dopamine D-2 receptor imaging agent. *J Nucl Med* 1990;31:648–654.
43. Kennedy L, Hanbauer I. Sodium-sensitive cocaine binding to rat striatal membrane: possible relationship to dopamine uptake sites. *J Neurochem* 1983;41:172–178.
44. Reith ME, Sershen H, Allen DL, Lajtha A. A portion of [^{3}H]cocaine binding in brain is associated with serotonergic neurons. *Mol Pharmacol* 1983;23: 600–606.
45. Boja J, Patel A, Carroll F, et al. Iodine-125-RTI-55: a potent ligand for dopamine transporters. *Eur J Pharmacol* 1991;194:133–134.
46. Scheffel U, Dannals R, Cline E, et al. Iodine-123/Iodine-125-RTI-55, an in vivo label for the serotonin transporter. *Synapse* 1992;11:134–139.
47. Staley JK, Basile M, Flynn DD, Mash DC. Visualizing dopamine and serotonin transporters in the human brain with the potent cocaine analogue [^{125}I]RTI-55: in vitro binding and autoradiographic characterization. *J Neurochem* 1994;62:549–556.
48. Little K, Kirkman J, Carroll F, Breese G, Duncan G. Iodine-125-RTI-55 binding to cocaine-sensitive dopaminergic and serotonergic uptake sites in the human brain. *J Neurochem* 1993;61:1996–2006.
49. Richfield E. Quantitative autoradiography of the dopamine uptake complex in rat brain using [^{3}H] GBR 12935: binding characteristics. *Brain Res* 1991; 541:1–13.
50. Hensler J, Ferry R, Labow D, Kovachich G, Frazer A. Quantitative autoradiography of the serotonin transporter to assess the distribution of serotonergic projections from the dorsal raphe nucleus. *Synapse* 1994;17:1–15.
51. Hyttel J. Citalopram: pharmacological profile of a specific serotonin uptake inhibitor with antidepressant activity. *Prog Neuropsychopharmacol Biol Psychiatry* 1982;6:277–295.
52. Biegon A, Dillon K, Volkow N, Hitzemann R, Fowler J, Wolf A. Quantitative autoradiography of cocaine binding sites in human brain postmortem. *Synapse* 1992;10:126–130.
53. Madras B, Fahey M, Bergman J, Canfield D, Spealman R. Effects of cocaine and related drugs in nonhuman primates. I. [^{3}H]Cocaine binding sites in caudate-putamen. *J Pharmacol Exp Ther* 1989;251:131–141.
54. Farde L, Halldin C, Muller L, Suhara T, Karlsson P, Hall H. PET study of [^{11}C]β-CIT binding to monoamine transporters in the monkey and human brain. *Synapse* 1994;16:93–103.
55. Laruelle M, Giddings S, Zea-Ponce Y, et al. Methyl 3β-(4-[^{125}I]iodophenyl) tropane-2β-carboxylate in vitro binding to dopamine and serotonin transporters under "physiological" conditions. *J Neurochem* 1994;62:978–986.
56. Bredberg E, Tedroff J, Aquilonius S, Paalzow L. Pharmacokinetics and effects of levodopa in advanced Parkinson's disease. *Eur J Clin Pharmacol* 1990;39:358–389.
57. Cortes R, Soranoi E, Pazos A, Probst A, Palacios J. Autoradiography of antidepressant binding sites in the human brain: localization using [^{3}H]imipramine and [^{3}H]paroxetine. *Neuroscience* 1988;27:473–496.
58. Dahlström A, Fuxe K. Evidence for the existence of monoamine-containing neurons in the central-nervous system. I. Demonstration of monoamines in the cell bodies of brain stem neurons. *Acta Physiol Scand* 1964;62:1–55.
59. Felten D, Laties A, Carpenter M. Monoamine-containing cell bodies in the squirrel monkey brain. *Am J Anat* 1974;139:153–166.
60. Laruelle M, Vanisberg M-A, Maloteaux J-M. Regional and subcellular localization in human brain of [^{3}H] paroxetine binding, a marker of serotonin uptake sites. *Biol Psychiatry* 1988;24:299.
61. Bäckström I, Bergström M, Marcusson J. High affinity [^{3}H] paroxetine binding to serotonin uptake sites in human brain tissue. *Brain Res* 1989;486: 261–268.
62. De Keyser J, De Baecker J, Ebinger G, Vauquelin G. [^{3}H]GBR 12935 binding to dopamine uptake sites in the human brain. *J Neurochem* 1989;53: 1400–1404.